

Design of narrow-band dielectric frequency-selective surfaces for microwave applications

ISSN 1751-8725
Received on 19th June 2014
Revised on 11th September 2015
Accepted on 29th September 2015
doi: 10.1049/iet-map.2015.0121
www.ietdl.org

Angela Coves¹ ✉, Stephan Marini², Benito Gimeno³, Daniel Sánchez⁴, Ana Rodríguez⁴, Vicente E. Boria⁴

¹Departamento de Ingeniería de Comunicaciones, Universidad Miguel Hernández de Elche, Spain

²Departamento de Física, Ingeniería de Sistemas y Teoría de la Señal, Universidad de Alicante, E-03690 Alicante, Spain

³Departamento de Física Aplicada, Instituto de Ciencia de Materiales, Universidad de Valencia, E-46100 Burjassot, Spain

⁴Departamento de Comunicaciones, Instituto de Telecomunicaciones y Aplicaciones Multimedia, Universidad Politécnica de Valencia, E-46022 Valencia, Spain

✉ E-mail: angela.coves@umh.es

Abstract: Two types of narrow-band dielectric frequency-selective surfaces (DFSSs) have been designed at microwave frequencies. First, a DFSS showing total reflection has been analysed under guided-mode resonance conditions, based on a single dielectric grating which is illuminated by a TM polarised two-dimensional plane wave at Brewster-angle incidence, presenting extremely low-reflectance sidebands adjacent to the resonance peak. Second, a DFSS exhibiting total transmission at normal TE incidence has been designed, by superimposing the resonance condition of a dielectric grating on the classical high-reflectance response of a periodic (band-gap based) structure formed by alternating homogeneous dielectric layers. Finally, the oblique incidence and polarisation effects on the spectral response of the designed DFSSs have been also studied. In addition, dielectric ohmic losses and the problem of the finite size of the periodic structures have been accounted for in both structures. The obtained results have been successfully validated with the commercial software tool high frequency structure simulator.

1 Introduction

Multilayered periodic structures can be designed to show total reflection or transmission under plane-wave excitation in the microwave-frequency [1–5] and optical-frequency [6–10] ranges, thus acting as band-stop or band-pass filters, respectively. In particular, narrow band reflection dielectric frequency-selective surfaces (DFSSs), with symmetrical line-shape in a limited spectral region, have already been demonstrated at optical frequencies. This study was based on single dielectric waveguide gratings (DWGs), and was developed at normal plane-wave incidence. The presented results were achieved by choosing the grating thickness to be near a multiple of half-wavelength (i.e. the resonance wavelength) in the layer, showing relatively low-reflectance sidebands [6, 7]. Alternatively, high-efficiency DFSS with extremely low-reflectance sidebands for a broad spectral region have been proposed in the optical range, based on a single DWG for a TM polarised plane wave (i.e. with its magnetic field parallel to the dielectric bars) at Brewster-angle incidence (defined for the equivalent homogeneous dielectric layer with average relative dielectric permittivity) [11–13]. On the other hand, a DWG embedded in a high/low multilayer dielectric structure can be used to obtain high-efficiency transmission DFSS, given that the thicknesses and dielectric constants are chosen to yield high reflection outside the passband (i.e. high-reflection [HR] design). The side-bands of the structure can be made arbitrarily low and extended over a large frequency range by adding layers with dielectric constants and thicknesses obeying HR conditions [4]. Such phenomena have been recently studied as a mimic of induced electromagnetic transmittance. In [14], it has been experimentally observed photoinduced resonant transmission of light through a gold film deposited on a photoinduced diffraction grating, grown in a glass substrate near the gold film surface by an optical pump beam. Therefore, the use of all-dielectric gratings for these purposes looks promising. However, the application of DFSSs in the microwave range has hardly been explored [4, 15].

In this work we focus on the filtering applications of DFSSs at microwave frequencies, at which their practical implementation with a finite number of grating periods has been already demonstrated [4, 16], making them a feasible approach. Narrow band-stop filters (also known as notch filters) are commonly used in combination with ultra-wideband filters [17–19], since in this wide frequency range there are interferences with existing narrow-band applications which need to be eliminated. In this paper, we propose the integration of narrow band-stop DFSSs directly in the high end microwave communication system as an alternative way to effectively eliminate the interfering signals. Although antennas with integrated filtering elements have already been considered by other authors [20–23], the implementation of this all-dielectric wireless technology in satellite antenna systems, can take advantage of lower losses of dielectric materials at such frequencies. In fact, the proposed systems might be implemented in both high gain ground based antennas and ground based radomes. On the other hand, narrow band-pass DFSSs can be used to transmit narrow-band applications, thus avoiding radiating interferences to other systems [24].

Specific designs of single-layer and multilayer narrow-band reflection and transmission DFSSs, using dielectric constants corresponding to practical materials commonly employed at microwave frequencies, are given in Sections 2 and 3, respectively. In both cases, the oblique incidence and polarisation effects, as well as the dielectric losses on the spectral response of the structures, have also been studied. To validate the results obtained with an in-house developed code, they have been successfully compared with the commercial software tool high frequency structure simulator (HFSS) [25] based on finite element, integral equation or advanced hybrid methods. In addition, in order to explore the problem of finding the size for a grating to provide an ideal filtering response, a study of the variation of the reflectance of the Brewster angle based reflection DFSS has been performed with an increasing number of grating periods using HFSS. We have concluded that a real device composed of a

hundred grating periods will guarantee a good filter performance with high selectivity. This result is in agreement with previously published practical FSS radomes which are typically comprised of hundreds of elements and similar sizes.

2 Brewster angle based reflection DFSS

In this section, the design procedure of a high-efficiency reflection DFSS based on a single DWG for a TM polarised two-dimensional plane wave ($\phi = 90^\circ$) at Brewster-angle incidence θ_B [26] is described (see Fig. 1). It is well known that for a single homogeneous dielectric layer with equal permittivities of the surrounding media, the Fresnel TM reflection vanishes at Brewster-angle incidence, independently of the layer thickness and the operation frequency. Making use of the guided-mode resonance properties of DWGs, we have designed a reflection DFSS consisting of a single DWG in air under oblique plane-wave incidence. As it is shown in Fig. 1, the DFSS consists of two alternating dielectric bars with relative permittivities ϵ_{r1} and ϵ_{r2} surrounded by air ($\epsilon_{ra} = 1.0$), whose widths are fixed at $D/2$, where D is the period of the structure, h_p being its thickness. The DFSS can be excited by a plane-wave with either TE or TM polarisation (i.e. the incident electric field being perpendicular or parallel to the plane of incidence, respectively).

The spectral response of a DFSS under oblique plane-wave incidence has been obtained with a vectorial modal method previously developed by the authors [27, 28]. In such method, the vector wave equation satisfied by the transverse components of the magnetic field in the periodic medium is expressed as an eigenvalue problem, which is solved by the application of the standard Galerkin moment method. Once the electromagnetic fields in all homogeneous and periodic regions are known, the scattering parameters of the dielectric periodic structure are obtained by imposing the boundary conditions at the plane interfaces separating the constituent layers.

In a DFSS, the angular and spectral location of the resonances are determined by the grating parameters that make the phase-match condition to be met, while its bandwidth increases with the modulation of the dielectric permittivity of the grating [29]. This fact is due to increased leakage of the waveguide grating about the resonance frequency.

Fig. 2 shows with solid line the angular reflection response of the theoretically designed single-layer waveguide grating constituted by ideally lossless dielectric bars alternated with air, for a TM-polarised two-dimensional incident plane wave ($\phi = 90^\circ$) at a frequency of 8 GHz, having the following parameters: $D = 20.538$ mm, $\epsilon_{r1} = 1.0$, $\epsilon_{r2} = 2.59$ (Plexiglas), $l_1 = l_2 = D/2$, and $h_p = 7$ mm. The average relative dielectric permittivity of the waveguide grating is thus given by $\bar{\epsilon}_r = (\epsilon_{r1}l_1 + \epsilon_{r2}l_2)/D$, being in this case $\bar{\epsilon}_r = 1.795$. To validate these results, we have successfully compared in Fig. 2 the reflectance of the designed DFSS with that obtained with the commercial

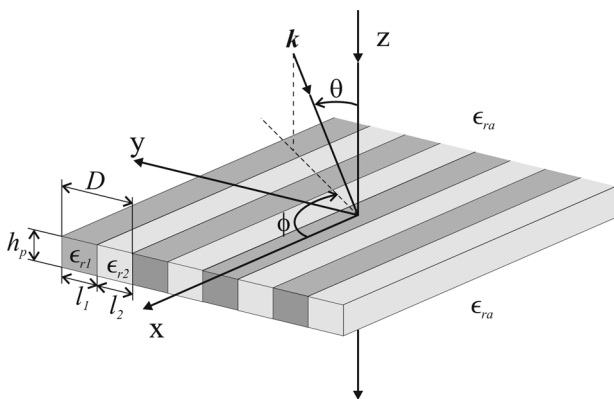


Fig. 1 DFSS with periodicity D in the Y direction, formed by two alternating dielectric bars homogeneous in the X axis

software tool HFSS based on the finite element method [25] (represented with circles). The computer time employed by the vectorial modal method was 0.56 s per point, while the computer time required by the HFSS code in the parametric sweep was 180.5 s per point. We have also represented in Fig. 2 (with dashed line) the electrical response of a homogeneous dielectric layer with $\epsilon_r = 1.795$ and the same thickness. The left-hand side inset gives an expanded view of the resonance response of the filter, with an angular width of 0.5° , which peaks at the Brewster angle $\theta_B = \arctan((\bar{\epsilon}_r)^{1/2}) = 53.26^\circ$. A contour plot of the reflectance of this structure around the resonance condition direction is shown in Fig. 3, where it can be observed that the structure resonates at the design angles $\theta_B = 53.26^\circ$ and $\phi = 90^\circ$, while the total reflection condition shifts to values of the angle θ above θ_B for decreasing values of ϕ . This behaviour could be used as a double angular tuning mechanism for a real device. The corresponding calculated frequency response obtained with the vectorial modal method, shown in Fig. 4 with solid line, reveals a single resonance peak response with extremely low-reflectance sidebands for a broad spectral region. The reflectance of the DFSS obtained with HFSS is again represented with points, while the spectral response of the equivalent homogeneous layer of $\epsilon_r = 1.795$ is also represented with dashed line. The right-hand side inset gives an expanded view of the electrical response, which resonates at a frequency of 8 GHz. It can be seen that at such frequency the Brewster-angle zero reflection is defeated by the resonance effect. Moreover, the resonance condition in this reflection DFSS is only achieved at Brewster angle for an azimuthal angle of incidence $\phi = 90^\circ$ (two-dimensional incidence), as it can be appreciated in Fig. 5, where it is represented the reflectance of the grating (solid line) at 8 GHz and θ_B (Brewster angle) as a function of the azimuthal angle ϕ , and also the reflectance of the equivalent homogeneous layer (dashed line).

Next, the effect of dielectric losses of the materials constituting the DWG in the spectral response has been also studied. To this end, the transmittance of the designed DFSS at θ_B and $\phi = 90^\circ$ is shown in Fig. 6 for different values of loss tangent of the dielectric bars (including, among them, the measured value of loss tangent of plexiglas at such frequencies [30], $\tan \delta = 0.0038$). In this figure, it can be observed that the resonance of the DFSS slightly broadens in frequency for increasing values of the loss tangent. Moreover, the transmittance minimum at resonance is less deep, as it is expected [4].

Finally, another aspect to be considered in this kind of structures is that, due to the physics of the guided-mode resonance, one of the problems is the size the grating must have to provide an ideal filtering response. This has somewhat been explored in [31, 32]. To explore the problem of finding the size for a DWG to provide an ideal filtering response, a study of the variation of the

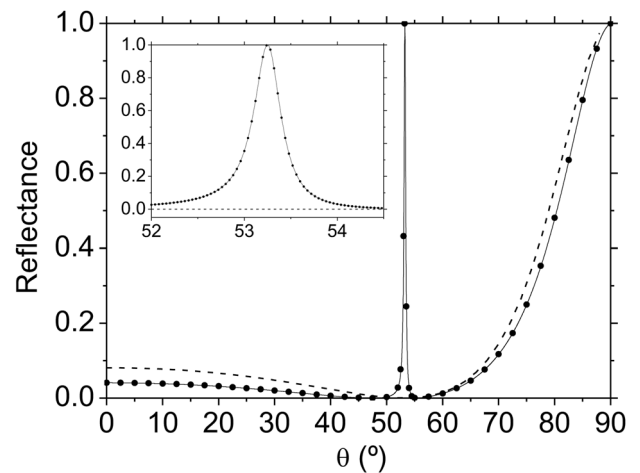
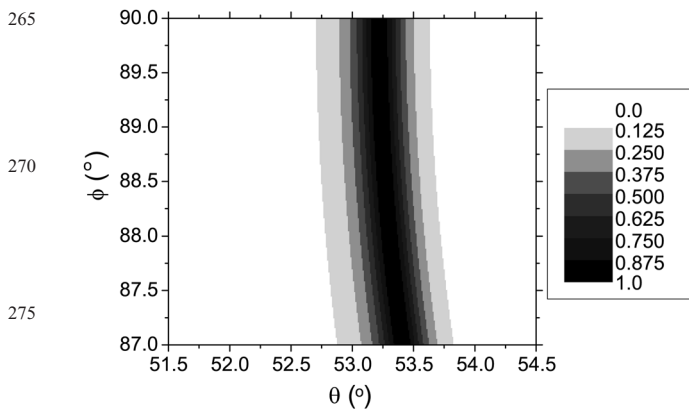


Fig. 2 Angular response (solid line) of a DFSS consisting of a single-layer DWG surrounded by air for a TM-polarised two-dimensional incident plane wave ($\phi = 90^\circ$) at a frequency of 8 GHz



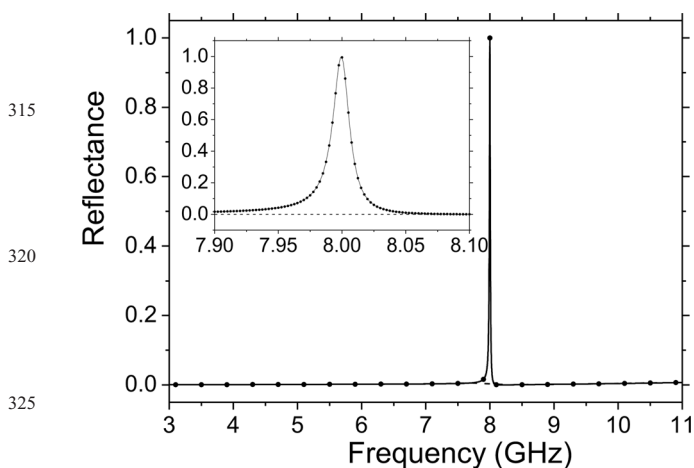
265
270
275
280 **Fig. 3** Contour plot of the reflectance of the reflection DFSS given in Fig. 2 for a TM-polarised wave around the resonance condition direction

reflectance of the proposed Brewster angle based reflection DFSS has been performed with an increasing number of grating periods. To this end, the reflectance under plane-wave incidence of a finite size DFSS formed by N periods with identical parameters to that of the infinite structure analysed in Fig. 2 has been calculated with HFSS. In Fig. 7 it is shown the reflectance of the finite DFSS case at θ_B and $\phi = 90^\circ$ around its resonance frequency for a different number N of periods ranging from 10 to 60 periods. Although the simulator was not able to analyse finite DFSS with more than 60 periods with sufficient accuracy due to the amount of required RAM, at the sight of the obtained results, we can conclude that a real device composed of one hundred grating periods will guarantee a good filter performance with high selectivity. This result is in agreement with previously published practical FSS radomes which are typically comprised of hundreds of elements and similar sizes [33–35].

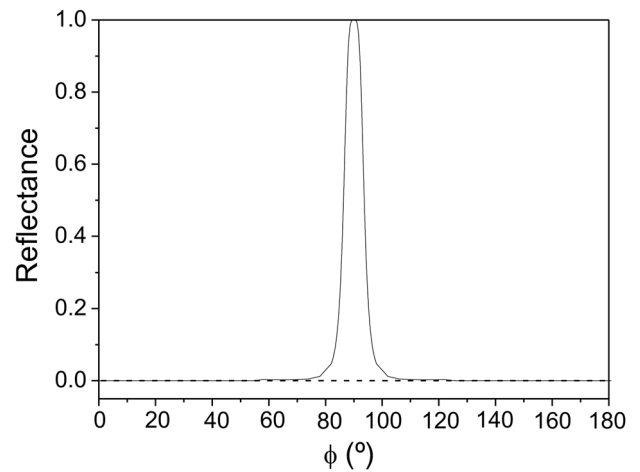
285
290
295
300 In conclusion, a high-efficiency reflection DFSS has been theoretically demonstrated at the Brewster angle, where the TM reflection is classically prohibited.

3 Band-gap based transmission DFSS

305 DWGs have been widely employed as reflection DFSSs [6, 27], but fewer implementations of transmission DFSSs have been achieved. In [8], thin-film multilayer structures incorporating a grating layer are used in the design of a transmission DFSS. Similarly, in [4] a transmission DFSS is designed by superimposing the resonance of a waveguide grating on the HR response of a high/low



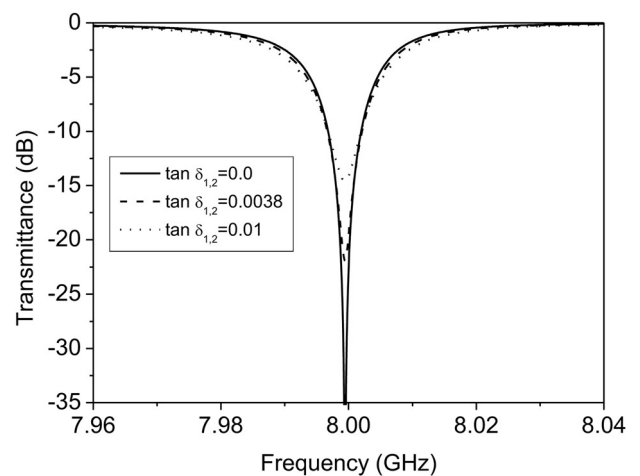
315
320
325
330 **Fig. 4** Spectral response of the reflection DFSS given in Fig. 2 for a TM-polarised wave incident at an angle $\theta_B = 53.26^\circ$ and $\phi = 90^\circ$ (solid line)



335
340
345 **Fig. 5** Reflectance of the reflection DFSS given in Fig. 2 (solid line) and of the equivalent homogeneous layer (dashed line) as a function of the azimuthal angle ϕ , for a three-dimensional TM-polarised wave at a frequency of 8 GHz that is incident at an angle $\theta = \theta_B$

quarter-wave thin-film stack. In this section, it is shown that highly efficient transmission DFSSs can be realised making use of the electromagnetic band-gap (EBG) properties of periodic structures. In particular, a single DWG is embedded in a multilayer dielectric structure, so that the guided-mode resonance of the DWG is superimposed on the high-reflectance response of the high/low multilayer stack.

355
360
365
370
375 In [36] it was described the analysis procedure for obtaining the dispersion diagram of periodic DFSSs under oblique two-dimensional plane-wave excitation. Here we have taken advantage of the dispersion diagram (shown in Fig. 5 of [36]) of an EBG material formed by alternating homogeneous dielectric layers of relative permittivities $\epsilon_{rh1} = 2.5$ and $\epsilon_{rh2} = 1.0$ and thicknesses $h_{h1} = h_{h2} = 5$ mm under normal TE plane-wave incidence, which means in this case that the electric field is parallel to the x axis. This infinite periodic lattice exhibits a first forbidden band in the 10–13.2 GHz frequency range. Based on the spectral response of a finite length implementation of such EBG lattice constituted by 9 high/low blocks in the z direction (see Fig. 8), we have replaced the central high index layer by a DWG with the same average relative permittivity and thickness, having the following parameters: $\epsilon_{rp1} = 1.0$, $\epsilon_{rp2} = 4.0$ (Taconic RF-41 [37]), $l_1 = l_2 = D/2 = 12.5$ mm. The transmittance response of the



380
385
390
395 **Fig. 6** Transmittance of the structure given in Fig. 2 (in dB) at θ_B and $\phi = 90^\circ$ for different values of loss tangent of the dielectric materials of the grating

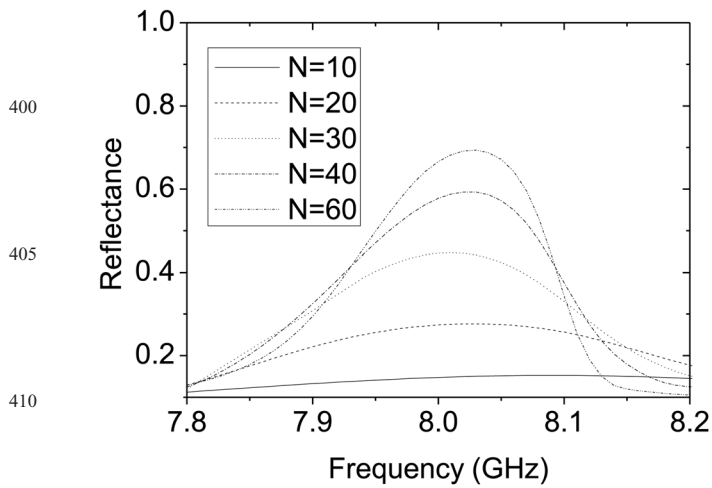


Fig. 7 Reflectance under plane-wave incidence at θ_B and $\phi = 90^\circ$ of a finite size DFSS formed by N periods with identical parameters to that of the infinite structure analysed in Fig. 2

homogeneous multilayer stack under normal plane wave incidence with TE polarisation is shown in Fig. 9 with dashed line, while the transmittance of the equivalent multilayer system with the embedded DWG is represented in the same figure with solid line. Since this multilayer waveguide-grating structure supports several guided modes, multiple resonance peaks are observed. It can be appreciated that there is one transmission peak centred at 11.77 GHz with extremely low sidebands in the 10.94–12.8 GHz frequency band. This extremely low level of out of band response cannot be achieved with conventional FSSs. Therefore, the mentioned resonance peak has a very large stop-band, which might be exploited as a narrow-band transmission DFSS for broadcasting satellite services operating in the Ku-band.

Previous studies on DWGs reveal that very small deviations from normal incidence can change qualitatively the spectral response of this kind of structures [28, 38]. In Fig. 10 it is shown the effect of varying the angle of incidence in the transmittance response around the resonance peak of Fig. 9 centred at 11.77 GHz (computed at normal incidence). The oblique incidence has two main effects on the spectral response of the embedded DWG: on one hand, additional resonance peaks appear next to the normal-incidence resonance peak. This effect is due to the break

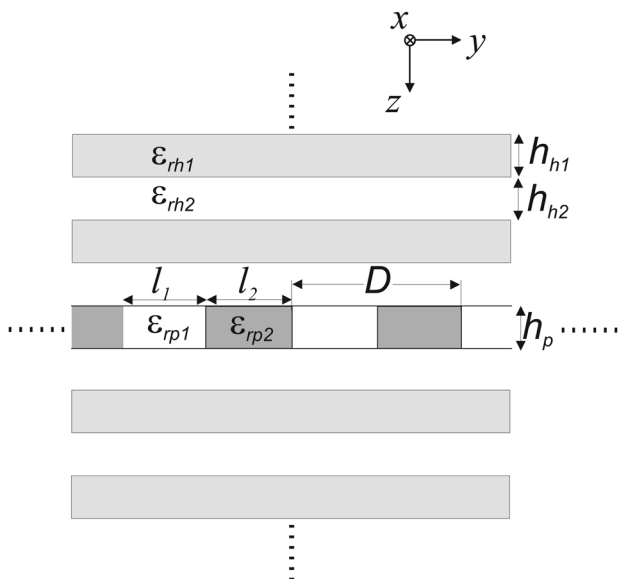


Fig. 8 DWG embedded in a high/low multilayer dielectric structure

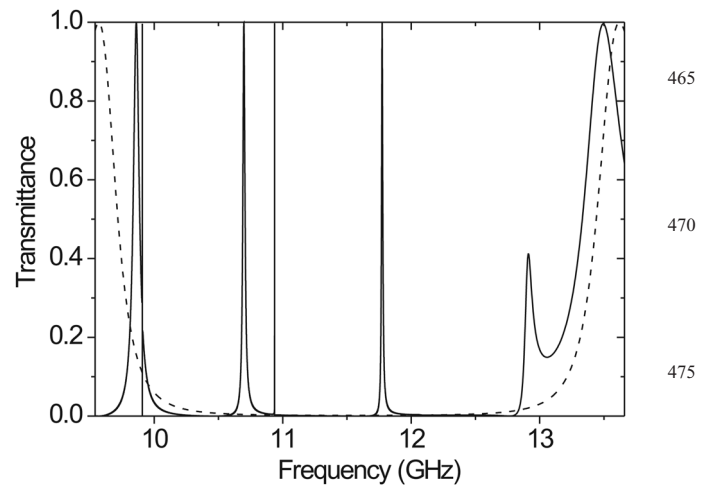


Fig. 9 Transmittance under normal TE incidence of an EBG lattice constituted by 9 high/low blocks of homogeneous dielectric layers (dashed line), and of the equivalent multilayer system with the central homogeneous layer replaced by a DWG (solid line)

of symmetry that the oblique incidence produces in the phase matching condition for the propagating and counter-propagating Bloch waves of the DWG [4]. On the other hand, for small angle variations (see the comparison between angles $\theta = 0^\circ$ and 1°), the resonance frequency slightly shifts with the angle θ as shown in Fig. 10. This second effect can be exploited as a mechanism for the tuning of the resonances appearing in such structure through small variations of the angle of incidence of the source. However, this is not valid for high values of the angle of incidence (see Fig. 10 for $\theta = 5^\circ$ or 10°), for which the structure under study no longer resonates at such particular frequency, due to the overall thickness of the proposed structure (whose electrical length is 3.53λ at this frequency).

For this filter, a study of the effect of ohmic losses of the materials in the transmittance of the resonance peak has also been performed. Fig. 11 shows the transmittance of the resonance peak of Fig. 9 centred at 11.77 GHz at normal incidence for different values of loss tangent of the dielectric material, showing that the resonance transmission peak decreases rapidly with the loss tangent, as it is commented in [4]. On the other hand, the finite size of the DWG embedded in the high/low multilayer stack will have a similar effect in the transmittance of the filter, that is, a broadening and reduction of the peak transmittance. However, it has been demonstrated [16] that the higher the dielectric contrast is in the periodic cell, the less periods are needed in order to achieve the

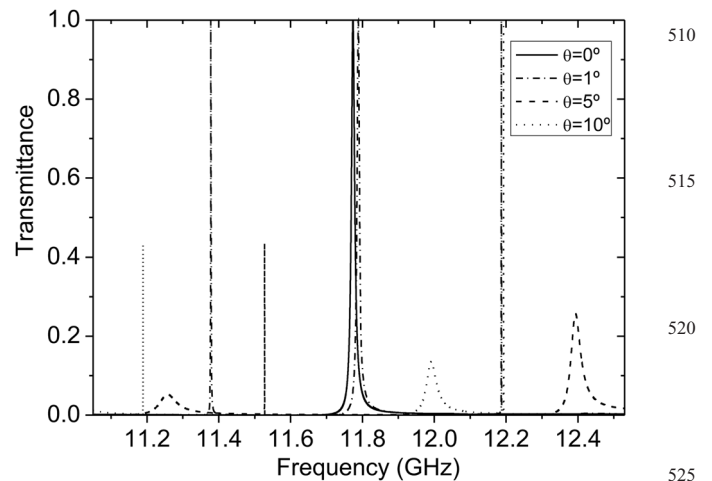


Fig. 10 Transmittance spectra of an embedded DWG at oblique incidence for several angles of incidence θ and $\phi = 90^\circ$

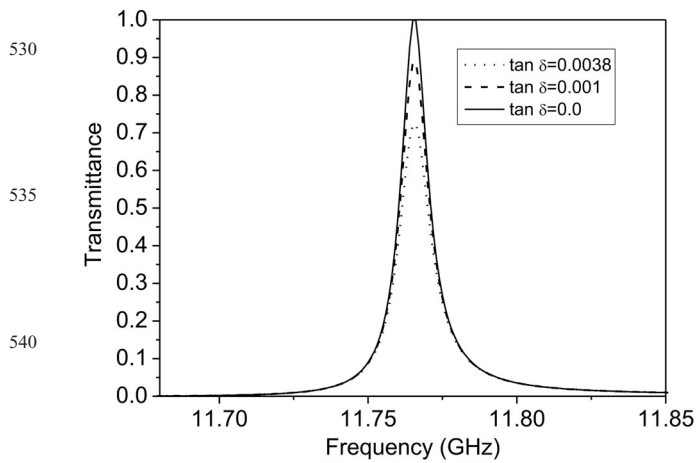


Fig. 11 Transmittance of the resonance peak of Fig. 9 centred at 11.77 GHz at normal incidence for different values of loss tangent of the dielectric materials

performance of the equivalent infinitely periodic structure. Thus, the selection of the high and low-index materials employed in the periodic cell of the DWG in this case (with $\epsilon_{rp1} = 1.0$ and $\epsilon_{rp2} = 4.0$) guarantees a good performance of the filter with fewer periods than those required in the first filter.

4 Conclusions

Specific designs of single-layer and multilayer narrow-band DFSSs have been successfully presented. On the one hand, a reflection DFSS based on a single dielectric grating has been designed for TM incidence at the Brewster angle where reflection is classically prohibited, showing low-reflectance sidebands adjacent to the resonance peak induced by the Brewster effect. On the other hand, a band-gap based transmission DFSS for normal TE incidence with extremely low sidebands has been designed. For this purpose, a dielectric grating has been embedded into a high/low multilayer dielectric structure, thus superimposing the considered resonance on the first stopband of a finite length implementation of the periodic lattice. This configuration gives rise to a practically zero transmittance out of the resonance peaks which cannot be obtained with conventional FSSs. The oblique incidence and polarisation effects on the spectral response of the designed DFSSs have been also studied. The obtained results have been successfully validated through comparisons with data from the commercial software tool HFSS. Finally, dielectric losses and finite size effects have been also accounted for in both cases.

5 Acknowledgments

This work was supported in part by Ministerio de Economía y Competitividad (MINECO) under Coordinated Project TEC2013-47037-C5.

6 References

- 1 Delihacioglu, K.: 'Frequency selective surfaces with multiple-strip group elements', *IEEE Antennas Wirel. Propag. Lett.*, 2012, **11**, pp. 1370–1373
- 2 Huang, X.J., Yang, C., Lu, Z.H., *et al.*: 'A novel frequency selective structure with quasi-elliptic bandpass response', *IEEE Antennas Wirel. Propag. Lett.*, 2012, **11**, pp. 1497–1500
- 3 Chiu, C.N., Wang, W.Y.: 'A dual-frequency miniaturized-element FSS with closely located resonances', *IEEE Antennas Wirel. Propag. Lett.*, 2012, **12**, pp. 163–165
- 4 Tibuleac, S., Magnusson, R., Maldonado, T.A., *et al.*: 'Dielectric frequency selective structures incorporating waveguide gratings', *IEEE Trans. Microw. Theory Tech.*, 2000, **4**, (4), pp. 553–561

- 5 Deng, F., Yi, X.Q., Wu, W.: 'Design and performance of a double-layer miniaturized-element frequency selective surface', *IEEE Antennas Wirel. Propag. Lett.*, 2013, **12**, pp. 721–724
- 6 Wang, S.S., Magnusson, R.: 'Design of waveguide-grating filters with symmetrical line shapes and low sidebands', *Opt. Lett.*, 1994, **19**, (12), pp. 919–921
- 7 Tibuleac, S., Magnusson, R.: 'Reflection and transmission guided-mode resonance filters', *J. Opt. Soc. Am. A*, 1997, **14**, (7), pp. 1617–1626
- 8 Tibuleac, S., Magnusson, R.: 'Diffraction narrow-band transmission filters based on guided-mode resonance effect in thin-film multilayers', *IEEE Photon. Technol. Lett.*, 1997, **9**, (4), pp. 464–466
- 9 Wang, S.S., Magnusson, R., Bagby, J.S., *et al.*: 'Guided-mode resonances in planar dielectric-layer diffraction gratings', *J. Opt. Soc. Am. A*, 1990, **7**, (8), pp. 1470–1474
- 10 Moharam, M.G., Gaylord, T.K.: 'Diffraction analysis of dielectric surface-relief gratings', *J. Opt. Soc. Am.*, 1982, **72**, (10), pp. 1385–1392
- 11 Magnusson, R., Shin, D., Liu, Z.S.: 'Guided-mode resonance Brewster filter', *Opt. Lett.*, 1998, **23**, (8), pp. 612–614
- 12 Shin, D., Liu, Z.S., Magnusson, R.: 'Resonant Brewster filters with absentee layers', *Opt. Lett.*, 2002, **27**, (15), pp. 1288–1290
- 13 Fu, X., Yi, K., Shao, J., *et al.*: 'Design of internal Brewster guided-mode resonance filter', *Chin. Opt. Lett.*, 2009, **7**, (6), pp. 462–464
- 14 Smolyaninov, I.I., Hung, Y.J., Davis, C.C.: 'Light-induced resonant transmittance through a gold film', *Appl. Phys. Lett.*, 2005, **87**, pp. 041101–041103
- 15 Zappelli, L.: 'Analysis of modified dielectric frequency selective surfaces under 3-D plane wave excitation using a multimode equivalent network approach', *IEEE Trans. Antennas Propag.*, 2009, **57**, (4), pp. 1105–1114
- 16 Barton, J.H., Garcia, C.R., Berry, E.A., *et al.*: 'All-dielectric frequency selective surface for high power microwaves', *IEEE Trans. Antennas Propag.*, 2014, **62**, (7), pp. 3652–3656
- 17 Ghazali, A.N., Pal, S.: 'Microstrip based UWB filter with controllable multiple notches and extended upper stopband'. Int. Conf. on Emerging Trends in Communication, Control, Signal Processing and Computing Application C2SPCA, 2013, pp. 1–5
- 18 Kurra, L., Abegaonkar, M.P., Basu, A., *et al.*: 'A compact uniplanar EBG structure and its application in band-notched UWB filter', *Int. J. Microw. Wirel. Tech.*, 2013, **5**, (4), pp. 491–498
- 19 Luo, X., Ma, J.G., Ma, K., *et al.*: 'Compact UWB bandpass filter with ultra narrow notched band', *IEEE Microw. Wirel. Compon. Lett.*, 2010, **20**, (3), pp. 145–147
- 20 Shambavi, K., Alex, Z.C.: 'Printed dipole antenna with band rejection characteristics for UWB applications', *IEEE Trans. Antennas Propag.*, 2010, **9**, pp. 1029–1032
- 21 Sung, Y.: 'Triple band-notched UWB planar monopole antenna using a modified H-shaped resonator', *IEEE Trans. Antennas Propag.*, 2013, **61**, (2), pp. 953–957
- 22 Cifola, L., Gerini, G., Morini, A.: 'Design of a low profile phased array filter with frequency agility and wide spurious rejection band'. Seventh European Conf. Antennas and Propagation, Gothenburg, 2013, pp. 1196–1200
- 23 Luo, G.Q., Hong, W., Tang, H.J., *et al.*: 'Filter consisting of horn antenna and substrate integrated waveguide cavity FSS', *IEEE Trans. Antennas Propag.*, 2007, **55**, (1), pp. 92–98
- 24 Zaman, A.U., Kildal, P.-S., Kishk, A.A.: 'Narrow-band microwave filter using high-Q groove gap waveguide resonators with manufacturing flexibility and no sidewalls', *IEEE Trans. Compon., Packag. Manuf. Technol.*, 2012, **2**, (11), pp. 1882–1889
- 25 ANSYS HFSS (High Frequency Structure Simulator), version 15.0, Ansys, Inc., Canonsburg, PA USA
- 26 Ramo, S., Whinnery, J.R., Van Duzer, T.: 'Fields and waves in communication electronics' (John Wiley & Sons, 1994)
- 27 Coves, A., Gimeno, B., Gil, J., *et al.*: 'Full-wave analysis of dielectric frequency-selective surfaces using a vectorial modal method', *IEEE Trans. Antennas Propag.*, 2004, **52**, (8), pp. 2091–2099
- 28 Coves, A., Gimeno, B., San Blas, A.A., *et al.*: 'Three-dimensional scattering of dielectric gratings under plane-wave excitation', *IEEE Antennas Wirel. Propag. Lett.*, 2003, **2**, pp. 215–218
- 29 Coves, A., Gimeno, B., Andres, M.V., *et al.*: 'Analysis and applications of dielectric frequency-selective surfaces under plane-wave excitation', *IEEE AP-S Int. Symp.*, 2003, **2**, pp. 825–828
- 30 Conklin, G.E.: 'Measurement of the dielectric constant and loss tangent of isotropic films at millimeter wavelengths', *Rev. Sci. Instrum.*, 1965, **36**, (9), pp. 1347–1349
- 31 Barton, J.H., Rumpf, R.C., Smith, R.W.: 'All-dielectric frequency selective surfaces with few periods', *Progr. Electromagn. Res. B*, 2012, **41**, pp. 269–283
- 32 Boye, R.R., Kostuk, R.K.: 'Investigation of the effect of finite grating size on the performance of guided-mode resonance filters', *Appl. Opt.*, 2000, **39**, (21), pp. 3649–3653
- 33 Mittra, R., Prakash, V.V.S.: 'Analysis of large finite frequency selective surfaces embedded in dielectric layers', *IEEE AP-S Int. Symp.*, 2002, **2**, pp. 572–575
- 34 Raynes, D.L., Delap, J.: 'Design of a finite array with a radome incorporating a frequency selective surface', *EUCAP*, 2007, pp. 1–5
- 35 Abadi, M.H., Meng Li, S.M.A., Behdad, N.: 'Harmonic-suppressed miniaturized-element frequency selective surfaces with higher order bandpass responses', *IEEE Trans. Antennas Propag.*, 2014, **62**, (5), pp. 2562–2571
- 36 Coves, A., Marini, S., Gimeno, B., *et al.*: 'Full-wave analysis of periodic dielectric frequency-selective surfaces under plane wave excitation', *IEEE Trans. Antennas Propag.*, 2012, **60**, (6), pp. 2760–2769
- 37 Taconic Advanced Dielectric Division (Available at <http://www.taconic-add.com/pdf/rf43>.)
- 38 Coves, A., Gimeno, B., Andrés, M.V.: 'Oblique incidence and polarization effects in coupled gratings', *Opt. Express*, 2012, **20**, (23), pp. 25454–25460

MAP20150121

Author Queries

665 Angela Coves, Stephan Marini, Benito Gimeno, Daniel Sánchez, Ana Rodríguez, 730
Vicente E. Boria

Q1 Please provide volume number for ref. [34].

670 735

675 740

680 745

685 750

690 755

695 760

700 765

705 770

710 775

715 780

720 785

725 790